

AD-A240 393



MTL TR 91-16

AD

2

**DEFORMATION OF ISODAMP
(A POLYVINYL CHLORIDE-BASED ELASTOMER)
AT VARIOUS LOADING RATES**

D. P. DANDEKAR, J. L. GREEN, M. HANKIN,
A. G. MARTIN, W. WEISGERBER, and R. A. SWANSON
MATERIALS DYNAMICS BRANCH

May 1991

DTIC
SELECTE
AUG 29 1991
S B D

Approved for public release; distribution unlimited.



US ARMY
LABORATORY COMMAND
MATERIALS TECHNOLOGY LABORATORY

91-08905



U.S. ARMY MATERIALS TECHNOLOGY LABORATORY
Watertown, Massachusetts 02172-0001

The findings in this report are not to be construed as an official Department of the Army position, unless so designated by other authorized documents.

Mention of any trade names or manufacturers in this report shall not be construed as advertising nor as an official indorsement or approval of such products or companies by the United States Government.

DISPOSITION INSTRUCTIONS

Destroy this report when it is no longer needed.
Do not return it to the originator

Block No. 20

ABSTRACT

Elastomers are widely used for mitigating and blocking small amplitude and low frequency vibrations. There is an interest in utilizing this material in dynamic loading environments where it would be subjected to high strain rates and high pressures. Since a paucity of information about elastomers exists in this environment a study was initiated. The objective of the study was to determine how the shock absorbing property of Isodamp C-1002 is modified under high strain rates of deformation and high stresses. In this investigation measurements of elastic wave velocity and attenuation to 10 MHz were obtained using ultrasonic techniques. Stress-strain histories were measured at strain rates of 10^{-4} s^{-1} to 10^4 s^{-1} under uniaxial stress and uniaxial strain conditions. Measurements were also made at shock loading conditions; i.e., 10^6 s^{-1} under uniaxial strain and high stresses. Results of these experiments were used to determine elastic constants and attenuation coefficients of Isodamp, parameters for a nonlinear Kelvin Model as a function of strain rate, bulk moduli as a function of strain rate, and a compression relation for Isodamp under shock loading conditions.

CONTENTS

	Page
1. INTRODUCTION	1
2. MATERIALS	1
3. ELASTIC PROPERTIES	
Experiments and Apparatus	2
Results	3
Analysis	5
4. QUASI-STATIC AND HIGH STRAIN RATE COMPRESSION	
Experiments and Apparatus	7
Results	9
Analysis	14
5. SHOCK WAVE LOADING	
Experiments and Apparatus	17
Results	19
Analysis	20
Future Study	21
6. SUMMARY	21



Accession For	
NIIS GRA&I	<input checked="" type="checkbox"/>
DTIC TAB	<input type="checkbox"/>
Unannounced	<input type="checkbox"/>
Justification _____	
By _____	
Distribution _____	
Availability Codes	
Dist	Avail and/or Special
A-1	

1. INTRODUCTION

Elastomers, because of their frequency dependent complex elastic properties, are widely used for isolating and attenuating undesirable structural vibrations and as mitigating and blocking noise barriers. These conventional uses subject an elastomer to small amplitude and low frequency vibrations. Therefore, there is a paucity of information pertaining to deformations of elastomers under dynamic loading, i.e., at high strain rates and high stresses or pressures. Recent experiments have shown that the elastomers could be successfully used under dynamic loading condition. The present investigation was initiated to determine deformation behavior of a polyvinyl chloride based elastomer sold by the trade name Isodamp C-1002, hereafter referred to as Isodamp. In the present investigation mechanical properties of Isodamp have been determined under wide ranging rates of loading, i.e., 10^{-4} s^{-1} to 10^6 s^{-1} and under large and infinitesimally small strains. All experiments were conducted in the U.S. Army Materials Technology Laboratory (MTL) at ambient room temperature, i.e., $300 \text{ K} \pm 5 \text{ K}$. The experimental program on Isodamp consisted of measuring:

- Elastic wave velocities and attenuation coefficient of elastic wave as functions of frequency, which are representative of dynamic mechanical properties at high rates of loading 10^6 s^{-1} and infinitesimally small strains.
- Large quasi-static deformation at very low strain rates (10^{-4} s^{-1}) under uniaxial stress and uniaxial strain conditions.
- High strain rate deformation; i.e., $10^3 - 10^4 \text{ s}^{-1}$ to large strains under uniaxial stress and uniaxial strain conditions by means of a Hopkinson Bar apparatus.
- Shock loading; i.e., at 10^6 s^{-1} to moderate strains under uniaxial strain conditions but high stresses or pressures.

A brief description of Isodamp is given in section 2; descriptions of the experiments, the apparatus used, and the information obtained from the experiments with Isodamp are given in sections 3 through 5. Section 3 deals with the elastic properties of Isodamp as obtained from ultrasonic wave propagation experiments. Section 4 deals with deformation of Isodamp obtained from the experiments conducted under quasi-static loading to high strain rate loading conditions. Section 5 deals with the deformation of Isodamp observed under plane shock wave loading conditions. Finally, section 6 summarizes the results of the present investigation pertaining to mechanical properties of Isodamp for ease of reference.

2. MATERIALS

Isodamp is manufactured by Cabot Corporation, Indianapolis, IN. It is sold in various forms, shapes, and differing compositions in terms of additives. Isodamp used in the present investigation belongs to the C-1000 series and is marketed as Isodamp C-1002. C. Byrne and her coworkers* determined that Isodamp is a polyvinyl chloride-based elastomer, containing two plasticizers: 2-ethylhexyl diphenyl phosphate, and bis (2-ethylhexyl) phthalate. Its pliable,

*BYRNE, C., and ZUKAS, W. To be published in *Advances in Urethanes Science and Technology*, v. 11, Technomic Publishing Company.

rubber-like behavior can be attributed to the presence of these two plasticizers. The plasticizers account for 40% to 50% of the mass of Isodamp, balance being polyvinyl chloride. In addition, Isodamp was found to contain traces of Cu, Ti, and Sb. Its blue color is thought to be due to the presence of copper phthalocyanine blue. Ti as TiO_2 is a white pigment, and Sb in the form of SbO_3 is added as a flame retardant.

The density of Isodamp was found to be $1.289 \pm 0.001 \text{ Mg/m}^3$. Isodamp has two thermal transitions: one at 253 K due to plasticized polyvinyl chloride, and a second at 347 K due to regions of unplasticized polyvinyl chloride. Isodamp does not appear to be porous. Some of the properties of Isodamp as reported by its manufacturer are given in Table 1.

Table 1. PROPERTIES OF ISODAMP AS REPORTED BY ITS MANUFACTURER AT ROOM TEMPERATURE

Property	Units	Magnitude
Density	Mg/m^3	1.289
Hardness	Shore A	56.000
Bayshore resilience	% Rebound (first)	4.800
Tensile strength	MPa	10.800
Elongation	%	459.000
Tensile modulus	MPa	3.100
Glass transition temperature	K	253.000

3. ELASTIC PROPERTIES

Experiments and Apparatus

Since pliable elastomers show frequency dependent elastic properties, it was necessary to measure both the elastic wave velocities and attenuation of elastic wave amplitudes as a function of frequency in Isodamp.

For elastic constant determinations, phase velocities of ultrasonic waves are measured. Phase velocity is defined as the velocity of individual cycles in a continuous wave and is given as:

$$V = f\lambda = \omega / k \quad (1)$$

where V is the phase velocity, f is the frequency of the sound wave, λ is the wavelength, ω is the angular frequency $2\pi f$, and k is the wave number $(2\pi/\lambda)$. If the phase velocity is non-dispersive; (it does not vary with frequency in a material) then its elastic constants remain unchanged under static or dynamic loading conditions for infinitesimally small strains.

For these phase measurements, an image superposition method¹ similar to the pulse-echo overlap method² was used. This method employs bursts of ultrasonic vibrations rather than continuous waves. The bursts consist of a continuous wave amplitude modulated by sinusoidal pulses synchronized with the wave. The repetition rate of the pulses is 1/2048 times the frequency of the continuous wave. Along with the sinusoidal envelope of the pulses, their duration is made long enough to encompass many cycles of the wave in order to make it as monochromatic as possible. Images of the pulses are superposed by control of the timing of pulses relative to the timing of oscilloscope sweeps. The control of timing is done by means of digital circuitry.

Phase data are obtained by comparing the phase of individual cycles as they enter and as they leave a specimen. This is done by adjusting the advance of bursts applied to the specimen so that the lead time equals the travel time of individual cycles, then the images of individual cycles coincide as they are presented alternately on the oscilloscope.

These measurements are done with two pairs of transducers as nearly identical as possible. One pair is coupled together; the other pair is separated by and coupled to the specimen. One transducer of each pair is connected in parallel to the signal source. The other two transducers are connected to the two signal inputs of the oscilloscope through two preamplifiers.

The signal frequency is started at the lowest frequency at which the travel time equals one half cycle or one cycle. From that point, the frequency is gradually increased and recorded along with the number of cycles of delay needed to keep the images of specific cycles superposed. An additional record may be kept of the number of cycles needed to match the envelope of the burst for group velocity determination. Ultrasonic wave velocity were measured in the frequency range of 2 MHz to 10 MHz. Further details of this method are given in Reference 1.

Ultrasonic wave attenuation was measured by immersing Isodamp of 1.54, 2.88, 5.78, 6.38, and 12.18 mm thicknesses in water between two ultrasonic transducers, one for sending and the other for receiving wave. A 0.30 mm piece of Isodamp was used as a reference to cancel the effect of surface reflection. The method used to measure attenuation was as follows. First, a specimen was immersed in water and the observed ultrasonic pulse was adjusted to a given amplitude on an oscilloscope. Then, the specimen was replaced by the 0.3 mm reference Isodamp. The pulse amplitude was now large on the oscilloscope. This signal was reduced to the original amplitude (the given amplitude) by means of a calibrated attenuator. Then attenuation and frequency were recorded. Attenuation as a function of frequency was measured from 0.2 to 9 MHz.

Results

The results of ultrasonic wave velocity measurements show that the values of ultrasonic longitudinal wave velocity are independent of frequency in the range of 2 MHz to 10 MHz. The value of longitudinal wave velocity was determined to be 1.79 km/s \pm 0.04 km/s. Attempts to measure the shear wave velocity over the same range of frequency proved unsuccessful except at a single frequency (2.5 MHz). The value of shear velocity was determined to be 0.62 km/s \pm 0.02 km/s at 2.5 MHz. These values of ultrasonic wave velocities in conjunction with the value

1. MARTIN, A. G. *Phase Velocity Measurements in Dispersive Materials by Narrow-Band Burst Phase Comparison*. U.S. Army Materials Technology Lab, AMMRC TR 76-22, 1976.
2. PAPADAKIS, E. P. *J. Acoust. Soc. Am.*, v. 42, 1967, p. 1045.

of density of Isodamp permit calculations of its elastic constants. The values of these constants are given in Table 2.

Table 2. ADIABATIC ELASTIC CONSTANTS (IN UNITS OF GPa), POISSON'S RATIO AND ATTENUATION COEFFICIENT OF LONGITUDINAL WAVE (IN UNITS OF DB/MM/MHz) FOR ISODAMP AT ROOM TEMPERATURE

Entities	Value
Elastic constants	
Longitudinal	4.13 ± 0.18
Young's	1.42 ± 0.09
Bulk	3.47 ± 0.15
Shear	0.495 ± 0.032
Poisson's Ratio	0.432 ± 0.006
Attenuation Coefficient	1.44

Attenuations of ultrasonic longitudinal wave measured as a function of frequency in various thicknesses of Isodamp are shown in Figure 1. Figure 1 shows that the values of attenuation expressed as db/mm versus frequency for the thicknesses of Isodamp ranging from 1.5 mm to 12.2 mm lie on a single line within the scatter of measurement. The slope of attenuation versus frequency is found to be 1.44 db/mm MHz for Isodamp in the frequency range 0.2 MHz to 9 MHz.

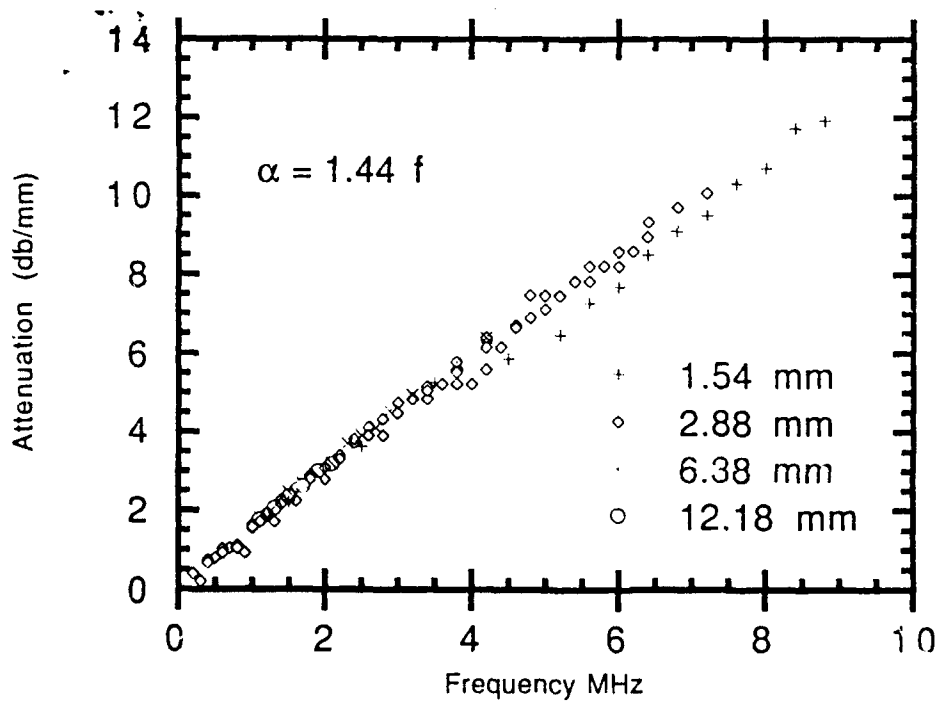


Figure 1. Attenuation of longitudinal ultrasonic waves in various thicknesses of Isodamp.

Analysis

We compared the value of shear modulus of Isodamp obtained from the measurement of ultrasonic shear wave velocity with the estimate of the modulus that can be obtained from the measurements of shear modulus of Isodamp between the angular frequency of 0.1 and 100 and over a temperature of 213 K to 314 K by Byrne and Zukas.* It is possible to make such an estimate because of a simple relationship that exists between the measurements of mechanical properties at various frequencies and at various temperatures of a simple linear viscoelastic material. This relationship takes a form:

$$G(\omega, T) = (\rho T / \rho_0 T_s) * G(\omega / a_T, T_s) \quad (2)$$

where $G(\omega, T)$ is the measure of mechanical property of interest at angular frequency ω and temperature T . Williams, Landel, and Ferry³ showed that the shift factor a_T in Equation 2 for most amorphous polymers may be written as

$$\log a_T = -8.86 (T - T_s) / [101.6 - (T - T_s)]. \quad (3)$$

In the above equations T_s is a characteristic temperature and ρ and ρ_0 are the density of the polymer at temperatures T and T_s , respectively.

Byrne and Zukas have applied the above frequency-temperature shift formalism to their shear modulus measurements with T_s equal to 294 K. Their measurements predict that the value of shear modulus of Isodamp at 2.5 MHz to be 0.4 GPa compared to the value of 0.495 ± 0.032 GPa obtained from the ultrasonic shear wave velocity measurement. It is not possible to comment upon the difference between these two estimates of the shear modulus of Isodamp because the precision of the measurements done by Byrne and Zukas is not known.

In what follows, an effort is made to determine the effect of nondispersion of longitudinal wave velocity and attenuation of longitudinal wave with frequency on the propagation of rectangular and ramp; i.e., sawtooth wave pulse of a few representative time durations. This was done by means of Fourier analysis,⁴ in which amplitude and frequency of the components of a given width of rectangular and sawtooth pulses of various time durations were determined. Then, for an assumed thickness of Isodamp, the attenuation of each component was used to calculate its amplitude. Finally, the components were added to produce the simulated output pulse. It should be noted that the analysis assumes a periodic applied pulse.

Figure 2 shows that a rectangular pulse travelling through 8 mm and 12 mm of Isodamp will spread out such that peak amplitude is reduced by 13% and 20%, from its original magnitude. Similarly, Figure 3 shows the attenuation of a triangular sawtooth pulse of 5 μ s duration propagation through Isodamp of various thicknesses. Figure 4 shows the change in shape and attenuation of the amplitude of sawtooth pulses of various duration, but unit magnitude propagating through 8 mm of Isodamp. These simulations are, of course, illustrative of the behavior of a small amplitude pulse as it propagates through Isodamp and they do not take into account effects of boundary condition on the propagating pulse. The results of the ultrasonic wave propagation measurements show

*BYRNE, C., and ZUKAS, W. To be published in *Advances in Urethanes Science and Technology*, v. 11, Technomic Publishing Company.

3. WILLIAMS, M. L., LANDEL, R. F., and FERRY, J. D. *J. Am. Chem. Soc.*, v. 77, 1955, p. 3701.

4. PIPES, L. A. *Applied Mathematics for Engineers and Physicists*. McGraw Hill, New York, NY, 1958.

that a longitudinal pulse of small amplitude is attenuated while transversing Isodamp and that the extent of attenuation is dependent upon both the thickness of Isodamp and width of the pulse. However, a large amplitude wave does not appear to be attenuated, as shown in the Shock Wave Loading Section, where the response of Isodamp under plane shock wave loading is presented.

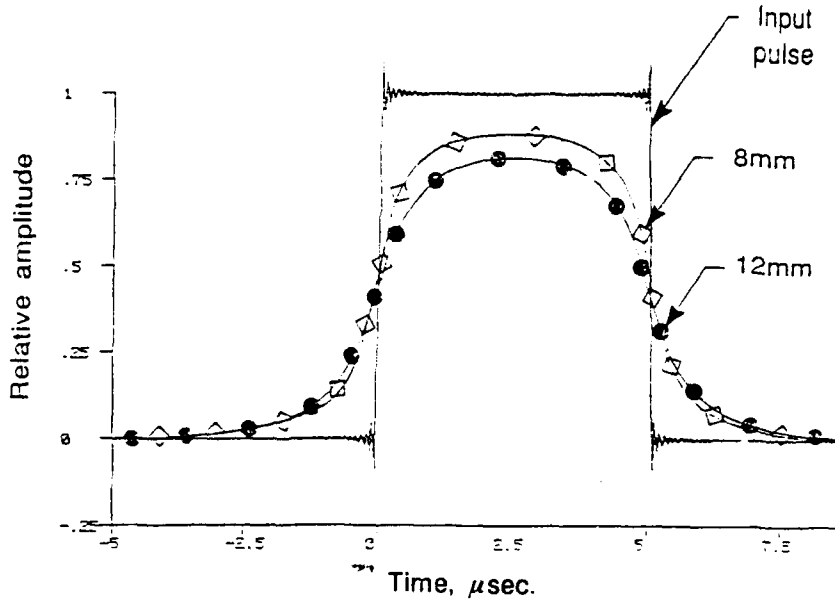


Figure 2. Simulated effect of a rectangular pulse transmitted through various thicknesses of Isodamp.

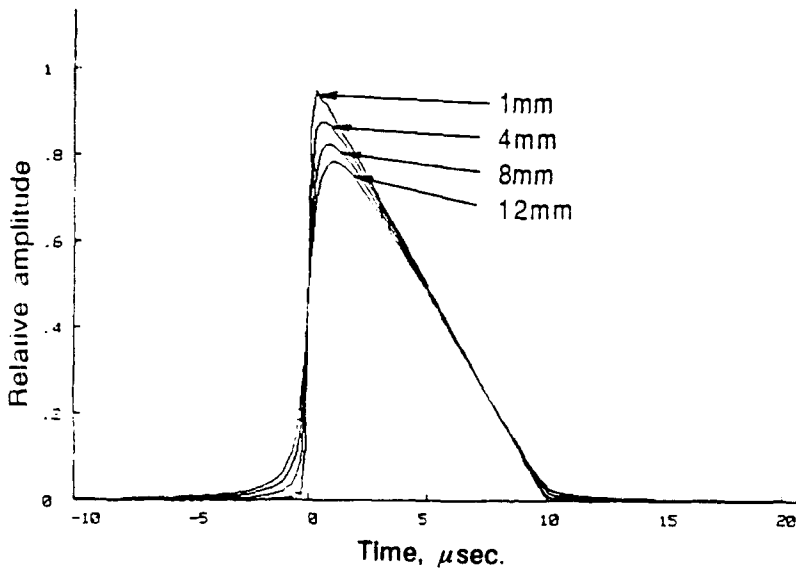


Figure 3. Simulated sawtooth pulse after travel through 1 mm, 4 mm, 8 mm, and 12 mm of Isodamp.

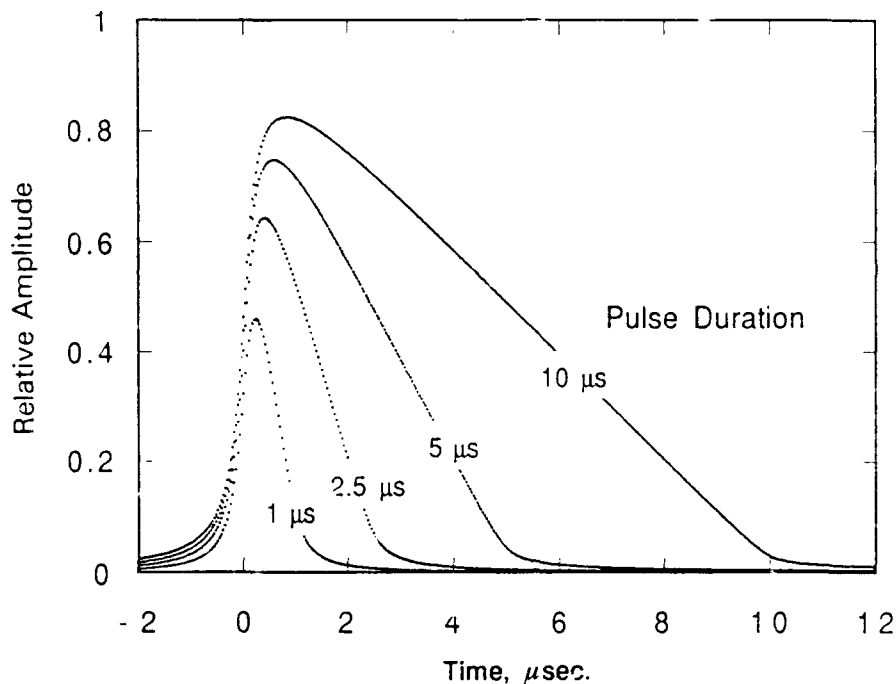


Figure 4. Simulation of effect of 8 mm of Isodamp on sawtooth pulses of unit amplitude.

4. QUASI-STATIC AND HIGH STRAIN RATE COMPRESSION

Experiments and Apparatus

This section deals with the experimental program to determine stress-strain histories of Isodamp under uniaxial compression at quasi-static and high rates of loading. Stress-strain histories were obtained under confined and unconfined configurations; i.e., under uniaxial stress and uniaxial strain conditions, respectively. A screw machine was used for static compression and a split Hopkinson pressure bar (SHPB) apparatus for high strain rate compression.

The quasi-static testing facility consists of a model 1125 Instron materials testing machine, associated instrumentation, and computer for data acquisition and analysis. All confined and unconfined static compression tests were conducted in crosshead control mode. The strain rate for these experiments was 10^{-4} /sec. The unconfined static compression specimens were right circular cylinders machined with ends flat and parallel, with nominal 12.7 mm diameter and 12.7 mm length. Both ends of specimen were lubricated with teflon tape. The unconfined specimens were loaded in compression until barreling occurred at which stage the test was discontinued. The load and displacement were monitored by computer and later converted to engineering stress and strain. The quasi-static confined compression specimens were injection molded right cylinders provided by Cabot Corporation. The specimen's nominal dimensions were 25.4 mm diameter by 12.7 mm length. The confinement rings were made of maraging 350 steel heat treated to HRC60 with a 25.4 mm inside diameter and a 1.59 mm wall thickness. The high strength steel rings were designed to remain elastic throughout the test providing uniform confinement

and a vehicle for determining the internal pressure in the ring. The external surface of the ring was instrumented with strain gages, and hoop strain measurements of the ring were made during the test. These measurements were easily related to hoop stress since the ring remained elastic and internal pressure was determined using thin wall cylinder methods.⁵ The steel pistons used for compressing Isodamp were machined with 0.0254 mm clearance of the ring, and had flat and parallel faces. During confined tests, load, displacements, and hoop strain were measured. The data were used to calculate volume change versus pressure for Isodamp.

High strain rate compression experiments on Isodamp were conducted by means of SHPB. A description of the SHPB apparatus at MTL is given in Reference 6. Basic principles underlying such an apparatus is that an elastic striker bar propelled by pressurized gas (nitrogen gas at MTL) to impact an elastic input bar, specimen, and an elastic output bar assembly. Stress (compressive) wave resulting due to impact propagates down the input bar. At the input bar specimen interface the stress wave is partly reflected and partly transmitted into the specimen. Since the incident bar is chosen, not only to be elastic but also of higher impedance than the specimen, the reflected wave is tensile in nature. The compressive wave transmitted through the specimen is transmitted into the output bar as a compressive wave. By measuring the magnitudes of strains generated in the input bar due to initial compressive wave and reflected tensile wave, and in the output bar due to transmitted compressive wave as a function of time, it is possible to obtain a stress-strain profile for the specimen. Specimen geometry is designed so as to deform it uniformly over the duration of measurement. The condition for uniform deformation of specimens has been extensively studied. These investigations suggest that to reduce the influence of longitudinal and radial inertia due to the rapid mass acceleration at high strain rates it is necessary that the ratio of length (L) and diameter (D) of a specimen should satisfy the following relation.⁷

$$L/D = (3\nu/4)^{0.5} \quad (4)$$

where ν is the Poisson's ratio of the specimen.

An additional condition suggested by Jashman⁸ is that for the time (τ) needed for the stress to attain first yield and for uniform deformation in a specimen of thickness (L) is given by

$$\tau = 5L/C, \quad (5)$$

where C is the elastic wave speed in the specimens. The value of τ should be as small as possible. However, the above equation is valid for a material which deforms plastically. There is no a prior argument to believe that a pliable elastomer will undergo a plastic deformation above a certain stress level. Hence, it was required to do a few preliminary experimentations to determine thickness of Isodamp specimens which should be used to assure uniform rate of deformation during the high rate of deformation using SHPB apparatus. The results of these experiments indicated that deformation of Isodamp was most uniform when specimens of 1.575 mm thickness were utilized. This yields a value of τ equal to 7.5 μ s and required that the value of D be equal to 2.77 mm. However, the high strain rate experiments conducted on Isodamp

5. TIMOSHENKO, S. *Strength of Materials, Part II*, D. Van Nostrand, New York, NY, 1936.

6. ROBERTSON, K. D., CHOU, S. C., and RAINEY, J. H. *Design and Operating Characteristics of a Split Hopkinson Pressure Bar Apparatus*. U.S. Army Materials Technology Lab, AMMRC TR 71-49, 1971.

7. DAVIES, E. D. H., and HUNTER, S. C. *J. Mech. Phys. Solids*, v. 11, 1963, p. 155.

8. JASHMAN, W. E. *J. Appl. Mech.*, v. 38, 1971, p. 75.

specimens were 1.575 mm thick and 6.35 mm in diameter because it was difficult to handle a 2.77 mm diameter specimen. This deviation from the required specimen dimension probably influenced the uniform rate of deformation of Isodamp as shown by the associated error bars on the measured strain rates and displayed in the figures of the following section.

SHPB was also used to determine compressions of Isodamp under confined condition to determine pressure versus volume change at high strain rates. The confined SHPB test used specimens that were the same diameter as bar with a close tolerance slip fit confinement ring over bar and specimen. The confinement rings were made of 6061-T6 aluminum. These rings had an outside diameter of 25.4 mm, and inner diameter of 12.7 mm, and a length of 17.5 mm. The inside and outside diameters were within ± 0.025 mm. In other words, the bar diameter and the inside diameter of the confinement rings differed by, at the most, 0.025 mm. The testing procedure was the same as those on unconfined SHPB tests except that striker velocity was much higher, and confinement ring hoop strain was also measured in addition to the strain gage outputs from input and output bars, as well as confinement ring strain gages. Since the confining ring prohibits the specimens expansion in a radial direction, the measureable axial deformation was a measure of approximate specimen volume change. The exact volume change of the specimen was calculated from the measured axial deformation and estimated change in the internal diameter of the confining ring due to the confining pressure. The maximum change in the diameter of the confining ring at 250 MPa is estimated to be 0.4%. These tests were found to measure change in length of specimen at a constant acceleration and not at a constant strain rate unlike the SHPB experiments under uniaxial stress condition.

Results

The results of compression experiments on Isodamp are presented as a function of strain rates under uniaxial stress and uniaxial strain conditions, respectively.

The stress-strain loci obtained under uniaxial stress conditions are shown in Figures 5 through 10. The observed scatter in the stress-strain loci are not uniform compression. Experiments conducted under quasi-static loading showed the least scatter. At high strain rates; i.e., the compression experiments conducted by using SHPB apparatus, the largest amount of scatter was evident in the results of experiments performed at $9400 \pm 100 \text{ s}^{-1}$ (see Figure 10); i.e., a scatter of ± 4 MPa is evident at almost all strain levels. The scatter in the compression experiments at other strain rates was around ± 2 MPa. The values of true stresses were calculated assuming that Isodamp suffers no volume change under uniaxial stress loading condition, consistent with the behavior of a rubber-like material. The largest strain measured in these experiments was 30%. These figures show that the strain rate influences the values of initial elastic modulus significantly. Finally, these data show that the stress-strain curves at strain rates larger than 5000 s^{-1} , Isodamp appear to indicate onset of plastic deformation at approximately 11% strain. However, this appearance of yield point in Isodamp is not accompanied with a permanent deformation or strain because recovered specimens are not found to be differing in their dimensions as compared to their respective initial dimensions. Slight downward shift in the stress-strain curves at higher strain rate shown in Figures 9 and 10 remain puzzling even though such tendency has been observed in deformation of polyvinyl chloride at high strain rates by Davies and Hunter.⁷ However, this overall deformation behavior of Isodamp can be reasonably reproduced by assuming applicability of a nonlinear Kelvin Model as done in the following subsection on analysis.

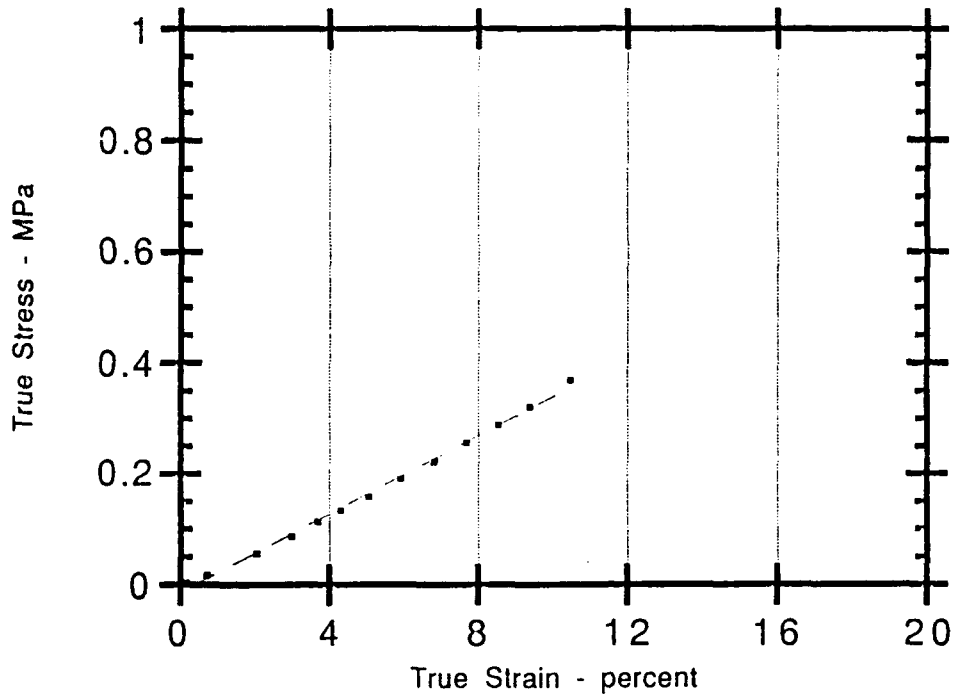


Figure 5. Quasi-static true stress - true strain curve for Isodamp under uniaxial stress conditions.

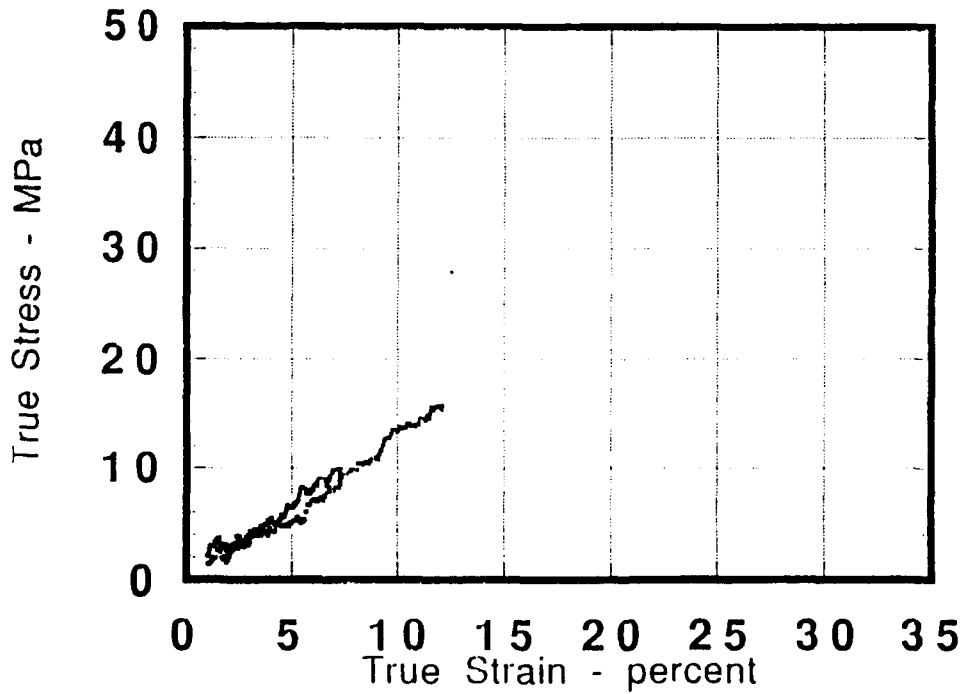


Figure 6. True stress - true strain curve for Isodamp under uniaxial stress conditions at $1.2 \times 10^3/\text{sec}$.

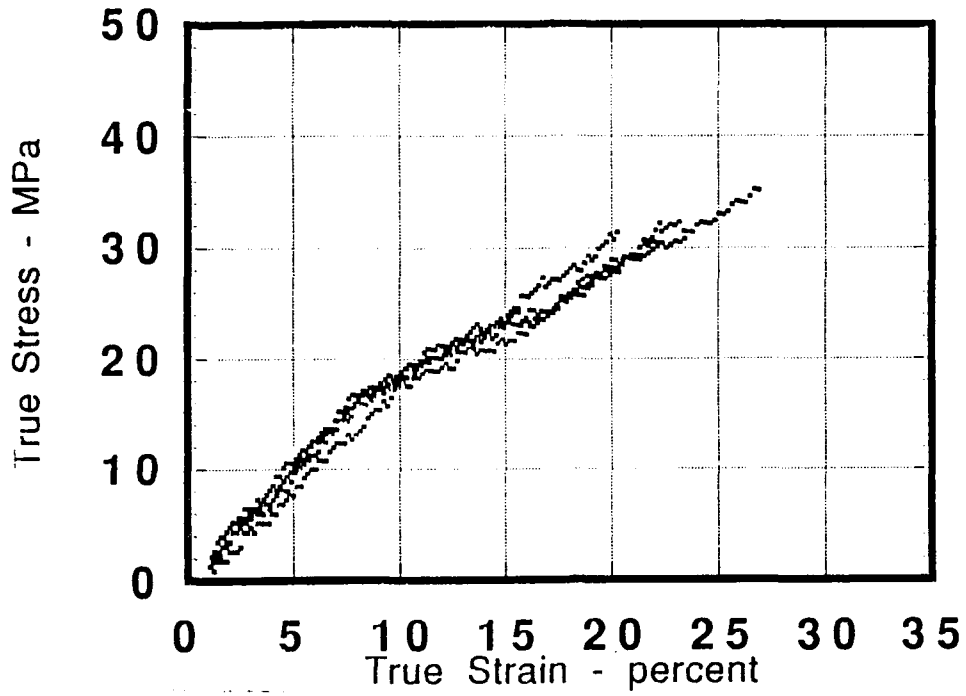


Figure 7. True stress - true strain curve for Isodamp under uniaxial stress conditions at 2.9×10^3 /sec.

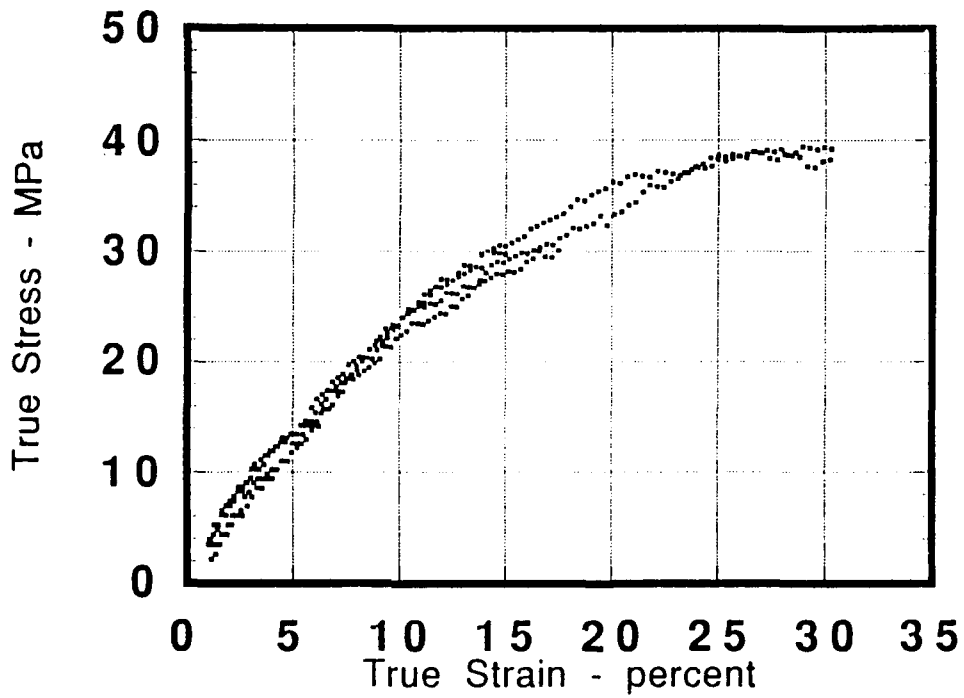


Figure 8. True stress - true strain curve for Isodamp under uniaxial stress conditions at 4.6×10^3 /sec.

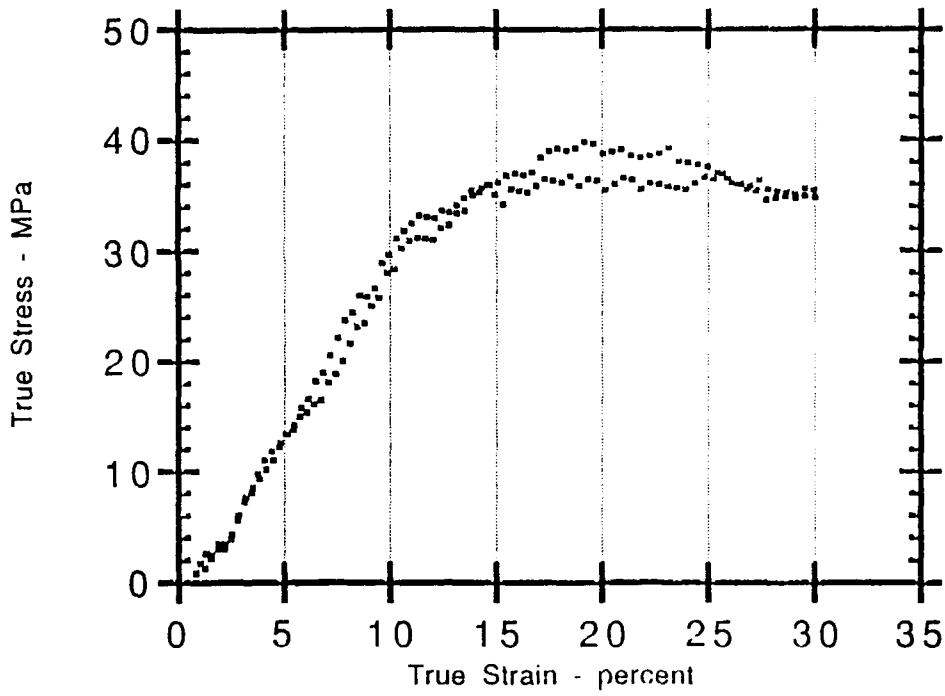


Figure 9. True stress - true strain curve for Isodamp under uniaxial stress conditions at $6.8 \times 10^3/\text{sec}$.

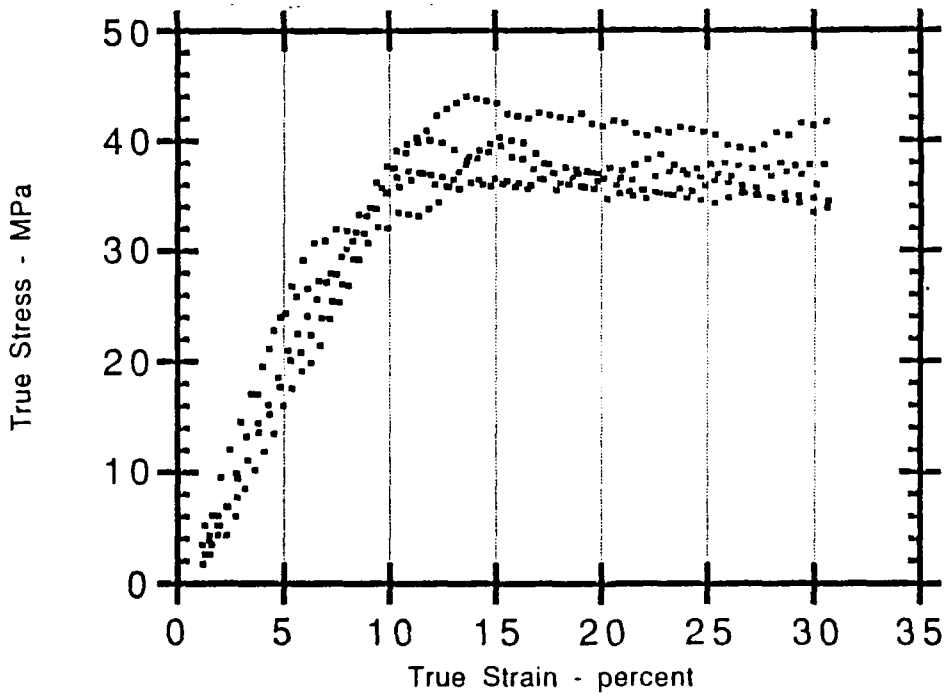


Figure 10. True stress - true strain curve for Isodamp under uniaxial stress conditions at $9.4 \times 10^3/\text{sec}$.

The stress-strain data obtained under confined loading condition; i.e., uniaxial strain condition is shown in Figure 11. In these experiments both the axial and radial stresses were simultaneously measured. The values of these stresses were found to be equal to one another within $\pm 2\%$ over the whole range of strain shown in Figure 11. This equality of axial and radial stresses suggest that Isodamp deforms like a fluid under uniaxial strain condition. Thus, the stress data gathered in these experiments are shown as pressure versus volume curves in Figure 11. Pressure volume data pertaining to a strain rate of 10^6 s^{-1} are from the shock wave experiment data given in the next section. The pressure-volume data are fairly linear to 6% volume change of Isodamp. The values of bulk moduli obtained from these experiments are given in Table 3. It should be noted that the strain rate observed during high strain rate compression using SHPB apparatus was not constant but varied linearly during these experiments. The strain rates given in the table and the figure are, therefore, an average rate. In other words, in these experiments the effect of inertial confinement caused a violation of the condition of uniform deformation for the Isodamp specimens. This table shows that the value of bulk modulus of Isodamp when deformed at even an average rate of 4100 s^{-1} equals that under the plane shock loading condition. However, the rate dependency of bulk modulus is significant going from quasi-static loading condition 10^{-4} s^{-1} to the strain rate of order of 10^3 s^{-1} . These results imply that volumetric compression data obtained at a single strain rate is not sufficient to describe compression behavior of Isodamp.

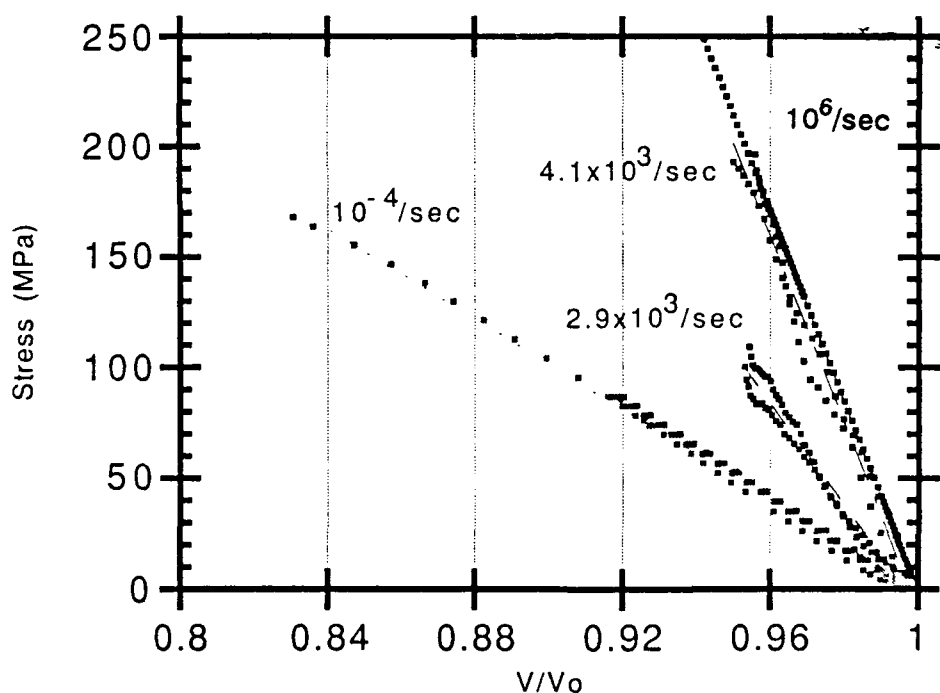


Figure 11. Confined compression of Isodamp at strain rates from $10^{-4}/\text{sec}$ to $10^6/\text{sec}$.

Table 3. VALUES OF INITIAL BULK MODULI (IN UNITS OF GPa) OF ISODAMP OBTAINED FROM UNIAXIAL STRAIN EXPERIMENTS AT VARIOUS RATES (sec⁻¹)

Strain Rate	Initial Bulk Modulus
1.0×10^{-4}	$1.02 \pm .008$
2.9×10^3	$2.30 \pm .013$
4.1×10^3	$4.21 \pm .021$
10^6	$3.86 \pm .013$

Analysis

There have been very few investigations reported in the literature dealing with the high strain rate compression of pliable elastomers; i.e., rubber-like materials. The models dealing with the large extensions of these materials to 500% to 600% are developed by envisioning a random coil configuration of molecules which is maintained by weak forces between neighboring hydrogen atoms or molecular links. Thus, as a rubber extends under a tensile stress it undergoes a continuous change from the closely coiled configuration to a fully extended one involving rotation about single bonds in chain structure, as well as rotation of extended chains from their initially random directions into the direction of the applied stress. This model is clearly not suitable for describing a large compression of such a material. Since Isodamp is a complex material (composed of polyvinyl chloride and two types of plasticizers and a few other minor additives), the analysis of the data given in this section is attempted from rheological perspective.

There are two simple rheological models which describe deformation response of viscous fluids and materials like rubber; the Maxwell Model and Kelvin Model, respectively. The nature of stress-strain curve is shown in Figures 7 through 10, and absence of a permanent strain in the recovered specimens of Isodamp imply that the Kelvin Model is likely to be applicable to present work. This model requires that the relationship between stress and strain normalized by the observed strain rate in a given experiment must be linear; that is,

$$\sigma/\dot{\epsilon} = \zeta + k \epsilon/\dot{\epsilon} \quad (6)$$

However, that is not the case, especially at strain rates above 4500 s^{-1} , or beyond 10% of strain. It was, therefore, decided to assume that the parameter k in the above equation is a function of strain. When the above mentioned assumption is implemented, Equation 6 becomes

$$\sigma/\dot{\epsilon} = \zeta + k(\epsilon) \epsilon/\dot{\epsilon} \quad (7)$$

where

$$k(\epsilon) = a_1 + a_2 \epsilon \quad (8)$$

and Equation 7 becomes

$$\sigma/\dot{\epsilon} = \zeta + a_1 (\epsilon/\dot{\epsilon}) + a_2 (\epsilon/\dot{\epsilon})^2 \dot{\epsilon} \quad (9)$$

or

$$\sigma = \zeta \dot{\epsilon} + a_1 \epsilon + a_2 \epsilon^2 \quad (10)$$

The values of parameters ζ , a_1 , and a_2 obtained by applying the method of the least squares to the stress-strain data are shown in Table 4. The reasonableness of the fit can be gaged by the value of correlation coefficient R. Figures 12 and 13 shown plots of nonlinear Kelvin Model fit to stress-strain data obtained under uniaxial stress condition at strain rates of 4600 s^{-1} and 9400 s^{-1} . Hence, the compression of Isodamp under various strain rates under uniaxial stress condition may be represented by Equation 9 or Equation 10 with appropriate values of the parameters taken from Table 4.

Table 4. VALUES OF ζ , a_1 , a_2 , AND REASONABLENESS OF FIT AS MEASURED BY CORRELATION COEFFICIENT (R) FOR COMPRESSION OF ISODAMP UNDER UNIAXIAL STRESS CONDITION AT VARIOUS STRAIN RATES

Strain Rate	ζ (MPa sec)	a_1 (MPa)	a_2 (MPa)	R
2.9×10^3	0.725×10^{-3}	162 ± 4	152 ± 13	0.9886
4.6×10^3	0.138×10^{-3}	256 ± 3	904 ± 17	0.9955
6.8×10^3	-0.29×10^{-3}	383 ± 6	900 ± 19	0.9707
9.4×10^3	0.25×10^{-3}	388 ± 11	972 ± 34	0.9392

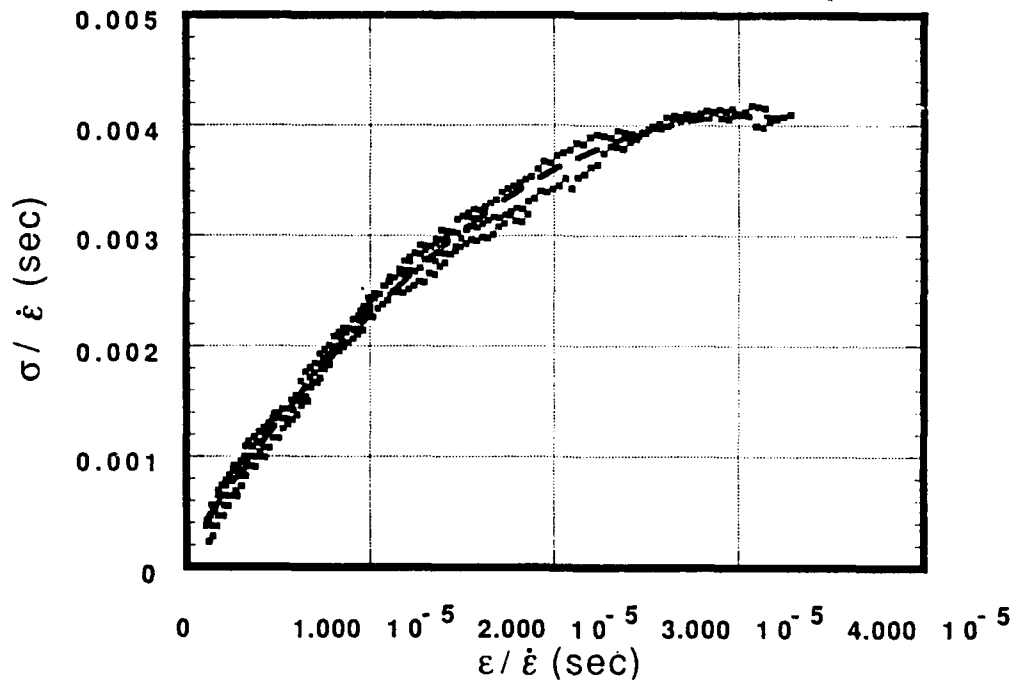


Figure 12. Nonlinear Kelvin Model fit of true stress true strain results at a strain rate of $4.6 \times 10^3/\text{sec}$.

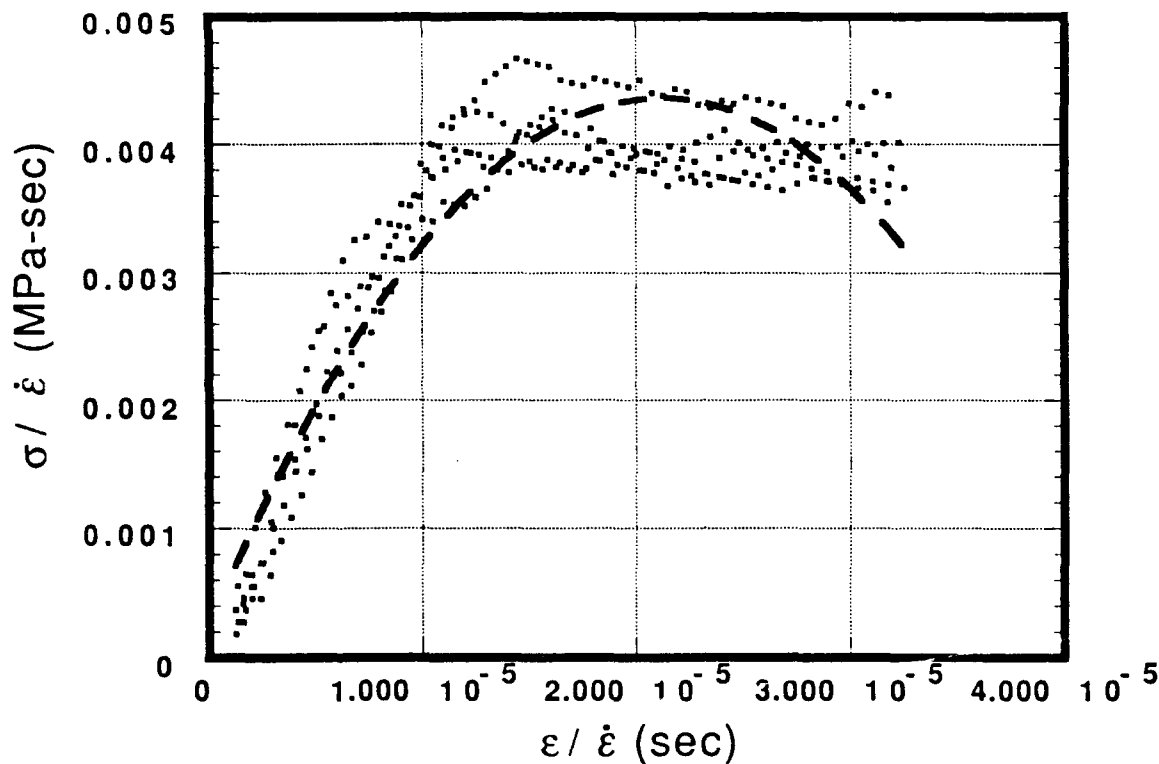


Figure 13. Nonlinear Kelvin Model fit of true stress true strain results at a strain rate of $9.4 \times 10^3/\text{sec}$.

It should be noted that the assumption of no volume change during compression under uniaxial stress condition implies that Equation 7 can be recast as

$$\sigma_x = \zeta \dot{\epsilon}_x + 2\mu(\epsilon_x) \epsilon_x \quad (11)$$

where x is the direction of compression and $\mu(\epsilon_x)$ is the strain dependent shear modulus.

If the lateral strains (ϵ_y and ϵ_z) are assumed to be uniform and isotropic, then we also have the following relation for both lateral strain rate ($\dot{\epsilon}_y$ and $\dot{\epsilon}_z$)

$$\dot{\epsilon}_y = \dot{\epsilon}_z = -2\mu(\epsilon_x) \epsilon_x / \zeta. \quad (12)$$

This provides a method to verify the model by measuring the lateral expansion of the specimen as a function of time and examine if the relation (see Equation 12) is satisfied. It should be possible to do this type of measurement with the aid of a streak camera.

In addition, the implication of the above assumed constitutive relation (Equation 7) when applied to compression experiments under uniaxial strain condition and where the axial

stress (σ_x) and the radial stress (σ_r) are found to be equal to one another (as is the case in the present investigation) is that:

$$P = \sigma_x = \sigma_r = \zeta \dot{\epsilon}_x / 3 + K(\epsilon_x) \epsilon_x \quad (13)$$

that is,

$$dP/d\epsilon_x = \zeta(d\dot{\epsilon}_x/d\epsilon_x) + K(\epsilon_x) + \epsilon_x [dK(\epsilon_x)/d\epsilon_x] \quad (14)$$

where P is the hydrostatic pressure and $K(\epsilon_x)$ is the strain dependent bulk modulus.

Equation 14 may be interpreted as follows: The effective bulk modulus of such a material is dependent upon ζ , $(d\dot{\epsilon}_x/d\epsilon_x)$, and $K(\epsilon_x)$. One can easily derive a few of the special cases of Equation 14. In the present case, as was mentioned earlier, the compression experiments under the uniaxial strain condition proceeded at a constant deceleration of strain rates. The values of the derivatives of the strain rate with respect to strain were found to be -8.59×10^4 and 1.257×10^5 for the average strain rates of 2.9×10^3 and 4.1×10^3 , respectively (see Figure 11 and Table 3). These values indicate that the contribution of the first term on the right-hand side of Equation 14, assuming a value of 10^{-3} for ζ (see Table 4), to respective bulk modulus is only 0.028 and 0.042 GPa at the average strain rate of 2.9×10^3 and 4.1×10^3 , respectively, and the observed constancy of the values of bulk modulus for a small volume change is consistent with the adopted constitutive model based upon the uniaxial stress-strain curve at high strain rates for Isodamp.

5. SHOCK WAVE LOADING

Experiments and Apparatus

Shock wave experiments were performed to determine response of Isodamp at extremely high rates of loading and high pressures but moderate strains. A part of the contents of this section has been published in Reference 9. These experiments were carried out using a 10 cm light gas gun which is capable of generating planar impacts with velocities ranging from 0.07 km/s to 0.7 km/s. Flyer plates are potted with epoxy in an aluminum ring which mounts in the front of a flat-nosed aluminum projectile. As the projectile emerges from the gun barrel, the aluminum flyer ring shorts out a series of charged pins which measure the projectile velocity. The flyer then impacts a target assembly which is similarly potted in a steel target ring. The target ring also incorporates flush charged pins which are used to indicate the time of impact and to trigger the recording oscilloscopes.

Two experimental configurations were used: One configuration of the Isodamp specimen is sandwiched between materials of higher shock impedance, causing several shocks to reverberate through the Isodamp, while the second configuration is a simple shock transmission. In the reverberation configurations, 6061-T6 aluminum, x-cut quartz, and Z-sapphire were used to generate successively increasing shocks through reverberation in Isodamp. Schematic configurations of reverberation shock experiments and a sketch of associated stress-particle velocity diagram are shown in Figure 14.

9. DANDEKAR, D. P., and HANKIN, M. *Shock Compression of Condensed Matter - 1989*. S. C. Schmidt, J. N. Johnson, and L. W. Davison, eds., Elsevier Science, New York, NY, v. 97, 1990.

Throughout this report, a reverberation configuration will be identified by the pair of materials used in the configuration; for example, Al-Al implies Isodamp sandwiched between two aluminum disks, etc. In the shock transmission configuration, an Isodamp flyer impacts an Isodamp target with manganin gages located 0.4 and 1.2 mm behind the impact surface.

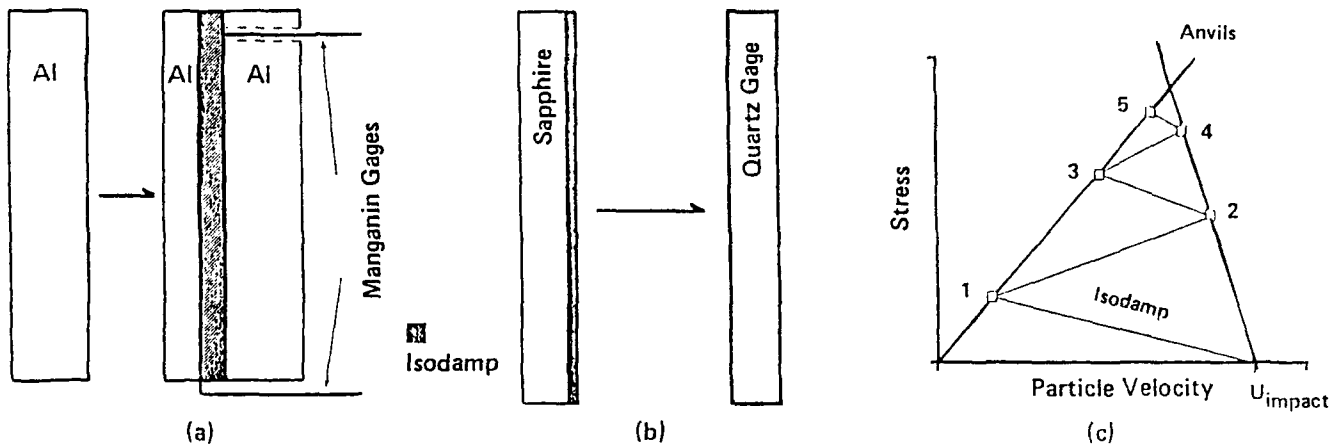


Figure 14.

- Schematic of reverberation experiments with two 6061-T6 Al (Al-Al) anvils.
- Schematic of reverberation experiments with Sapphire and Quartz (Sp-Qz) anvils.
- Schematic of stress - particle velocity states generated in such experiments. Measurable states in (a) are #'s 1-5 and in (b) are #'s 1, 3, and 5.

The Isodamp used in the shock experiments was obtained from the manufacturer in flat sheets of varying thicknesses. Due to its pliable nature, we found it impossible to lap the elastomer. The supplied sheets were quite flat, however, usually being parallel to within $20 \mu\text{m}$ over a 50 mm diameter. The 6061-T6 aluminum disks used in the Al-sandwich shots were lapped flat to within six to eight light bands and parallel to within $10 \mu\text{m}$. The quartz gages and sapphire disks used in the present study are supplied by the manufacturer flat to within five bands of sodium light and parallel to within $3 \mu\text{m}$. The Isodamp specimens in the first two configurations were quite thin; i.e., 0.4 mm, 0.8 mm, or 1.5 mm, allowing many shock reverberations to pass through the specimen before edge releases effected the one-dimensional strain conditions at the gage location. Impact velocity was measured using charged pins located just in front of the target. Stress-time profiles were obtained by using either manganin gages (Micomeasurments, Inc., Type LM-SS-125CH-048) or x-cut quartz gages. Manganin gages of the above type have been calibrated by Rosenberg, et al.¹⁰ In those experiments where x-cut quartz were used to record stress profile, the guard ring configuration and the calibration coefficient provided by Graham¹¹ were used. Since the impact time is known these stress-time profiles, along with measured impact velocity, yield three

10. ROSENBERG, Z., YAZIV, D., and PARTOM, Y. J. Appl. Phys., v. 51, 1980, p. 3702.
 11. GRAHAM, R. A. J. Appl. Phys., v. 46, 1975, p. 1901.

observable parameters; stress, impact velocity, and shock speed. The precisions of the stress and shock speed measurements are 2.5% and 4%, respectively, while the impact velocity is measured to within $\pm 0.1\%$.

Results

Results of seven reverberation and three transmission experiments performed on Isodamp are summarized in Table 5. It is clear from this table that all the possible shock reverberation states were not, or could not, be measured in these seven experiments either due to configuration of a specific experiment or due to gage failure.

Table 5. EXPERIMENTAL PARAMETERS

Expt. No.	Isodamp Specimen (mm)	Impact Velocity (km/s)	Shock States									
			1		2		3		4		5	
			Stress (GPa)	Particle Velocity (km/s)								
<u>Reverberation</u>												
Al-Al												
1	0.4	0.0725	-	-	0.2730	0.1107	-	-	0.4512	0.1693	-	-
2	1.5	0.0712	0.1663	0.0615	0.2662	0.1075	0.3624	0.1421	0.4292	0.1672	0.4774	0.1856
Sp-Qz												
3	0.4	0.3436	0.9166	0.2831	-	-	2.7033	0.6383	-	-	3.5460	0.7683
4	0.8	0.3436	0.8778	0.2857	-	-	-	-	-	-	-	-
5	0.4	0.3530	0.9604	0.2896	-	-	2.8374	0.6480	-	-	3.7009	0.7683
6	0.8	0.3530	0.9631	0.2895	-	-	2.8825	0.6447	-	-	-	-
7	0.4	0.1924	0.4563	0.1623	-	-	1.3493	0.3836	-	-	1.8575	0.4815
<u>Transmission</u>												
8	0.4	0.6034	0.9777	0.3017	n/a	n/a	n/a	n/a	n/a	n/a	n/a	n/a
9	0.4	0.6056	0.9817	0.3028	n/a	n/a	n/a	n/a	n/a	n/a	n/a	n/a

The results of two transmission experiments (8 and 9) and a reverberation experiment (5) show that there is no measurable attenuation of a shock pulse that propagates through Isodamp of thickness 0.4 mm. This may be inferred either from the values of impedances calculated from the measured values of stress and particle velocities at the impact surface of Isodamp in Experiment 5, and at the transmitted surface of Isodamp in the transmitted experiment, or from comparison of the value of calculated stress in Isodamp with a particle velocity of 0.3022 km/s and estimated impedance from Experiment 5; i.e., 1.002 GPa with the observed value of 0.9737 GPa. Also, Experiments 5 and 6 show that third shock states attained in 0.4 mm and 0.8 mm thick due to two reverberations from the first shock state are indistinguishable from one another. Similar observations can be made regarding the results of Experiments 1 and 2 where the impact velocities were close to one another. The shock and reshoock states attained in 0.4 mm and 1.5 mm thick Isodamp appear to be indistinguishable.

Thus, it could be concluded that the results of these experiments do not show evidence of stress attenuation of a relatively wide stress pulse during initial or subsequent reshocks.

The reverberation experiments were performed with two specific goals in mind: to reach higher shock stresses with impact velocity of less than 0.6 km/s, and to observe if any attenuation results in the shock stress state as shock reverberates through different thicknesses of Isodamp.

In the present series of experiments, highest stress reached 3.7 GPa. One question which naturally arises is what is the best way to represent the Hugoniot of Isodamp from the results of these experiments. Shock states are reached both from initially undeformed state of Isodamp and those attained from preshocked states.

The stress-particle velocity relations were derived from the shock states in Table 5. Equation 15 was derived for the initial undeformed state, the (σ, u) pairs listed under state 1 in Table 5. Equation 16 represents a similar relation between σ - u derived from all the shock states (σ, u) pairs listed in Table 5.

$$\sigma = 2.4152u + 2.7788u^2 \quad (15)$$

and

$$\sigma = 2.2308u + 3.2889u^2. \quad (16)$$

These relations imply that the estimates of σ from these equations differ by, at the most, 6% from one another when the value of u is less than or equal to 0.77 km/s.

These relations when expressed in terms of shock velocity (U) and particle velocity (u) are, respectively,

$$U = 1.8737 + 2.1558u \quad (17)$$

$$U = 1.7306 + 2.5515u. \quad (18)$$

To sum up, in the absence of any additional data either of these relations can be used for the purpose of calculations provided an accuracy of better than 6% is not desired in the calculation of stress from a given particle velocity. Finally, initial shock wave velocity of 1.87 in Isodamp is larger than the measured ultrasonic longitudinal wave velocity determined at 2.5 MHz. However, stress wave profiles did not show a presence of an elastic precursor.

Analysis

It is of interest to compare the shock deformation behaviors of polyvinyl chloride and Isodamp because such a comparison will allow recognizing the effect of plasticizers. The density of polyvinyl chloride is 1.376 Mg/m³. Its shock response is summarized by the following relation between its shock velocity and particle velocity;¹² that is,

$$U = 2.31 + 1.469u. \quad (19)$$

12. LASL Hugoniot Data, S. P. Marsh, ed., University of California Press, Berkeley, CA, 1980.

A consideration of the properties of polyvinyl chloride and Isodamp allows the following to be noted:

- The effect of adding plasticizers is to reduce both the density and the initial shock wave velocity in polyvinyl chloride from 1.376 Mg/m^3 to 1.289 Mg/m^3 for Isodamp and from 2.31 km/s to 1.87 km/s in Isodamp, respectively.
- The calculated values of the bulk moduli of polyvinyl chloride and Isodamp are 7.34 GPa and 4.50 GPa , respectively.
- The estimates of the pressure derivatives of the bulk moduli of polyvinyl chloride and Isodamp are 4.88 and 7.62 , respectively.

These results suggest that the effect of adding two plasticizers mentioned earlier to polyvinyl chloride is to make Isodamp more compressible than polyvinyl chloride at low stresses; i.e., $\leq 5.0 \text{ GPa}$, and to make Isodamp less compressible than polyvinyl chloride above 5.0 GPa .

Future Study

It is known that unloading of shock waves occur along an adiabatic path. Thus, observation of unloading behavior of Isodamp will permit determination of its equation of state. Shock transmission experiments with full release in Isodamp have been conducted to a peak pressure of 1.0 GPa . However, the data remain to be analyzed. In addition, it is necessary to validate the inference that Isodamp may be less compressible than polyvinyl chloride above 5.0 GPa by conducting appropriate shock experiments above this stress. These experiments will be performed in the near future.

6. SUMMARY

The results of ultrasonic wave velocity, attenuation, quasi-static and high strain rate compression, as well as shock wave experiments, permit the following general remarks about the deformation of Isodamp at room temperature.

- Magnitude of strain, strain rate, and type of confinement condition influence the deformation behavior of Isodamp. No single type of experiment is uniquely suited to determine compression behavior of Isodamp at room temperature.
- The infinitesimally small amplitude sinusoidal vibration packet or pulse is attenuated as it propagates through Isodamp. The attenuation depends upon both the thickness of Isodamp and the width of the pulse.
- Under unconfined conditions (under uniaxial stress condition), the compression of Isodamp may be represented by a nonlinear Kelvin Model and given by Equation 9 provided strain rate is between 2900 s^{-1} and 9400 s^{-1} and total strain is smaller than or equal to 30% .
- The quasi-static compressive behavior (under uniaxial stress condition), can be determined by using a value of 4.85 MPa for the shear modulus of Isodamp.

- Under confined condition (under uniaxial strain condition), the compression of Isodamp may be calculated by using the value of bulk modulus given in Table 3 consistent with the rate of compression provided the total strain is less than or equal to 6%.
- Under shock loading, the compression equation for Isodamp is given by

$$P = \rho_0 C_0^2 \eta / (1 - s \eta)^2 \quad (20)$$

where ρ_0 is the initial density, C_0 and s are, respectively, the intercept and the slope in Equation 18 and η is $(1 - \rho_0 / \rho)$.

- The values of shock velocity (C_0) 1.73 ± 0.04 km/s and the bulk sound velocity 1.64 ± 0.04 km/s obtained from the ultrasonic velocity measurements may be considered to be indistinguishable from one another.
- For a thickness up to 3 mm the amplitude of the shock wave did not attenuate as it propagated through the Isodamp, unlike in the case of ultrasonic wave propagation.
- Under quasi-static loading and uniaxial strain condition, the compression behavior is given by a constant value of bulk modulus (K); i.e., 1.02 GPa.

DISTRIBUTION LIST

No. of Copies	To
1	Office of the Under Secretary of Defense for Research and Engineering, The Pentagon, Washington, DC 20301
	Commander, U.S. Army Laboratory Command, 2800 Powder Mill Road, Adelphi, MD 20783-1145
1	ATTN: AMSLC-IM-TL
1	AMSLC-CT
	Commander, Defense Technical Information Center, Cameron Station, Building 5, 5010 Duke Street, Alexandria, VA 22304-6145
2	ATTN: DTIC-FDAC
1	MIAC/CINDAS, Purdue University, 2595 Yeager Road, West Lafayette, IN 47905
	Commander, Army Research Office, P.O. Box 12211, Research Triangle Park, NC 27709-2211
1	ATTN: Information Processing Office
	Commander, U.S. Army Materiel Command, 5001 Eisenhower Avenue, Alexandria, VA 22333
1	ATTN: AMCSCI
	Commander, U.S. Army Materiel Systems Analysis Activity, Aberdeen Proving Ground, MD 21005
1	ATTN: AMXSY-MP, H. Cohen
	Commander, U.S. Army Missile Command, Redstone Scientific Information Center, Redstone Arsenal, AL 35898-5241
1	ATTN: AMSMI-RD-CS-R/Doc
1	AMSMI-RLM
	Commander, U.S. Army Natick Research, Development and Engineering Center, Natick, MA 01760-5010
1	ATTN: Technical Library
	Commander, U.S. Army Satellite Communications Agency, Fort Monmouth, NJ 07703
1	ATTN: Technical Document Center
	Commander, U.S. Army Tank-Automotive Command, Warren, MI 48397-5000
1	ATTN: AMSTA-ZSK
2	AMSTA-TSL, Technical Library
	Commander, White Sands Missile Range, NM 88002
1	ATTN: STEWS-WS-VT
	President, Airborne, Electronics and Special Warfare Board, Fort Bragg, NC 28307
1	ATTN: Library
	Director, U.S. Army Ballistic Research Laboratory, Aberdeen Proving Ground, MD 21005
1	ATTN: SLCBR-TSB-S (STINFO)
	Commander, Dugway Proving Ground, Dugway, UT 84022
1	ATTN: Technical Library, Technical Information Division
	Commander, Harry Diamond Laboratories, 2800 Powder Mill Road, Adelphi, MD 20783
1	ATTN: Technical Information Office
	Director, Benet Weapons Laboratory, LCWSL, USA AMCCOM, Watervliet, NY 12189
1	ATTN: AMSMC-LCB-TL
1	AMSMC-LCB-R
1	AMSMC-LCB-RM
1	AMSMC-LCB-RP
	Commander, U.S. Army Foreign Science and Technology Center, 220 7th Street, N.E., Charlottesville, VA 22901-5396
3	ATTN: AIFRTC, Applied Technologies Branch, Gerald Schiesinger

No. of Copies	To
1	Commander, U.S. Army Aeromedical Research Unit, P.O. Box 577, Fort Rucker, AL 36360 ATTN: Technical Library
1	Commander, U.S. Army Aviation Systems Command, Aviation Research and Technology Activity, Aviation Applied Technology Directorate, Fort Eustis, VA 23604-5577 ATTN: SAVDL-E-MOS
1	U.S. Army Aviation Training Library, Fort Rucker, AL 36360 ATTN: Building 5906-5907
1	Commander, U.S. Army Agency for Aviation Safety, Fort Rucker, AL 36362 ATTN: Technical Library
1	Commander, USACDC Air Defense Agency, Fort Bliss, TX 79916 ATTN: Technical Library
1	Clarke Engineer School Library, 3202 Nebraska Ave. North, Ft. Leonard Wood, MO 65473-5000
1	Commander, U.S. Army Engineer Waterways Experiment Station, P. O. Box 631, Vicksburg, MS 39180 ATTN: Research Center Library
1	Commandant, U.S. Army Quartermaster School, Fort Lee, VA 23801 ATTN: Quartermaster School Library
1	Naval Research Laboratory, Washington, DC 20375 ATTN: Code 5830
2	Dr. G. R. Yoder - Code 6384
1	Chief of Naval Research, Arlington, VA 22217 ATTN: Code 471
1	Edward J. Morrissey, WRDC/MLTE, Wright-Patterson Air Force Base, OH 45433-6523
1	Commander, U.S. Air Force Wright Research & Development Center, Wright-Patterson Air Force Base, OH 45433-6523 ATTN: WRDC/MLLP, M. Forney, Jr.
1	WRDC/MLBC, Mr. Stanley Schulman
1	NASA - Marshall Space Flight Center, MSFC, AL 35812 ATTN: Mr. Paul Schuerer/EH01
1	U.S. Department of Commerce, National Institute of Standards and Technology, Gaithersburg, MD 20899 ATTN: Stephen M. Hsu, Chief, Ceramics Division, Institute for Materials Science and Engineering
1	Committee on Marine Structures, Marine Board, National Research Council, 2101 Constitution Ave., N.W., Washington, DC 20418
1	Librarian, Materials Sciences Corporation, 930 Harvest Drive, Suite 300, Blue Bell, PA 19422
1	The Charles Stark Draper Laboratory, 68 Albany Street, Cambridge, MA 02139
1	Wyman-Gordon Company, Worcester, MA 01651 ATTN: Technical Library
1	Lockheed-Georgia Company, 86 South Cobb Drive, Marietta, GA 30063 ATTN: Materials and Processes Engineering Dept. 71-11, Zone 54
1	General Dynamics, Convair Aerospace Division, P.O. Box 748, Fort Worth, TX 76101 ATTN: Mfg. Engineering Technical Library
2	Director, U.S. Army Materials Technology Laboratory, Watertown, MA 02172-0001 ATTN: SLCMT-TML
3	Authors

U.S. Army Materials Technology Laboratory
Watertown, Massachusetts 02172-0001
DEFORMATION OF ISODAMP (A POLYVINYL
CHLORIDE-BASED ELASTOMER) AT VARIOUS
LOADING RATES:
D. P. Dandekar, J. L. Green, M. Hankin, A. G. Martin,
W. Weisgerber, and R. A. Swanson

AD UNCLASSIFIED
UNLIMITED DISTRIBUTION
Key Words
High strain rate
Elastic constants
Attenuation

Technical Report MTL TR 91-16, May 1991, 25 pp-
illus-tables, D/A Project: 611102.H420011

Elastomers are widely used for mitigating and blocking small amplitude and low frequency vibrations. There is an interest in utilizing this material in dynamic loading environments where it would be subjected to high strain rates and high pressures. Since a paucity of information about elastomers exists in this environment a study was initiated. The objective of the study was to determine how the shock absorbing property of Isodamp C-1002 is modified under high strain rates of deformation and high stresses. In this investigation measurements of elastic wave velocity and attenuation to 10 MHz were obtained using ultrasonic techniques. Stress-strain histories were measured at strain rates of 10^{-4} s $^{-1}$ to 10^4 s $^{-1}$ under uniaxial stress and uniaxial strain conditions. Measurements were also made at shock loading conditions; i.e., 10^6 s $^{-1}$ under uniaxial strain and high stresses. Results of these experiments were used to determine elastic constants and attenuation coefficients of Isodamp, parameters for a nonlinear Kelvin Model as a function of strain rate, bulk moduli as a function of strain rate, and a compression relation for Isodamp under shock loading conditions.

U.S. Army Materials Technology Laboratory
Watertown, Massachusetts 02172-0001
DEFORMATION OF ISODAMP (A POLYVINYL
CHLORIDE-BASED ELASTOMER) AT VARIOUS
LOADING RATES:
D. P. Dandekar, J. L. Green, M. Hankin, A. G. Martin,
W. Weisgerber, and R. A. Swanson

AD UNCLASSIFIED
UNLIMITED DISTRIBUTION
Key Words
High strain rate
Elastic constants
Attenuation

Technical Report MTL TR 91-16, May 1991, 25 pp-
illus-tables, D/A Project: 611102.H420011

Elastomers are widely used for mitigating and blocking small amplitude and low frequency vibrations. There is an interest in utilizing this material in dynamic loading environments where it would be subjected to high strain rates and high pressures. Since a paucity of information about elastomers exists in this environment a study was initiated. The objective of the study was to determine how the shock absorbing property of Isodamp C-1002 is modified under high strain rates of deformation and high stresses. In this investigation measurements of elastic wave velocity and attenuation to 10 MHz were obtained using ultrasonic techniques. Stress-strain histories were measured at strain rates of 10^{-4} s $^{-1}$ to 10^4 s $^{-1}$ under uniaxial stress and uniaxial strain conditions. Measurements were also made at shock loading conditions; i.e., 10^6 s $^{-1}$ under uniaxial strain and high stresses. Results of these experiments were used to determine elastic constants and attenuation coefficients of Isodamp, parameters for a nonlinear Kelvin Model as a function of strain rate, bulk moduli as a function of strain rate, and a compression relation for Isodamp under shock loading conditions.

U.S. Army Materials Technology Laboratory
Watertown, Massachusetts 02172-0001
DEFORMATION OF ISODAMP (A POLYVINYL
CHLORIDE-BASED ELASTOMER) AT VARIOUS
LOADING RATES:
D. P. Dandekar, J. L. Green, M. Hankin, A. G. Martin,
W. Weisgerber, and R. A. Swanson

AD UNCLASSIFIED
UNLIMITED DISTRIBUTION
Key Words
High strain rate
Elastic constants
Attenuation

Technical Report MTL TR 91-16, May 1991, 25 pp-
illus-tables, D/A Project: 611102.H420011

Elastomers are widely used for mitigating and blocking small amplitude and low frequency vibrations. There is an interest in utilizing this material in dynamic loading environments where it would be subjected to high strain rates and high pressures. Since a paucity of information about elastomers exists in this environment a study was initiated. The objective of the study was to determine how the shock absorbing property of Isodamp C-1002 is modified under high strain rates of deformation and high stresses. In this investigation measurements of elastic wave velocity and attenuation to 10 MHz were obtained using ultrasonic techniques. Stress-strain histories were measured at strain rates of 10^{-4} s $^{-1}$ to 10^4 s $^{-1}$ under uniaxial stress and uniaxial strain conditions. Measurements were also made at shock loading conditions; i.e., 10^6 s $^{-1}$ under uniaxial strain and high stresses. Results of these experiments were used to determine elastic constants and attenuation coefficients of Isodamp, parameters for a nonlinear Kelvin Model as a function of strain rate, bulk moduli as a function of strain rate, and a compression relation for Isodamp under shock loading conditions.

U.S. Army Materials Technology Laboratory
Watertown, Massachusetts 02172-0001
DEFORMATION OF ISODAMP (A POLYVINYL
CHLORIDE-BASED ELASTOMER) AT VARIOUS
LOADING RATES:
D. P. Dandekar, J. L. Green, M. Hankin, A. G. Martin,
W. Weisgerber, and R. A. Swanson

AD UNCLASSIFIED
UNLIMITED DISTRIBUTION
Key Words
High strain rate
Elastic constants
Attenuation

Technical Report MTL TR 91-16, May 1991, 25 pp-
illus-tables, D/A Project: 611102.H420011

Elastomers are widely used for mitigating and blocking small amplitude and low frequency vibrations. There is an interest in utilizing this material in dynamic loading environments where it would be subjected to high strain rates and high pressures. Since a paucity of information about elastomers exists in this environment a study was initiated. The objective of the study was to determine how the shock absorbing property of Isodamp C-1002 is modified under high strain rates of deformation and high stresses. In this investigation measurements of elastic wave velocity and attenuation to 10 MHz were obtained using ultrasonic techniques. Stress-strain histories were measured at strain rates of 10^{-4} s $^{-1}$ to 10^4 s $^{-1}$ under uniaxial stress and uniaxial strain conditions. Measurements were also made at shock loading conditions; i.e., 10^6 s $^{-1}$ under uniaxial strain and high stresses. Results of these experiments were used to determine elastic constants and attenuation coefficients of Isodamp, parameters for a nonlinear Kelvin Model as a function of strain rate, bulk moduli as a function of strain rate, and a compression relation for Isodamp under shock loading conditions.